Journal of Applied Research in Water and Wastewater

E-ISSN: 2476-6283

Journal homepage: https://arww.razi.ac.ir

Optimal redesign of urban surface water collection network using hybrid SWMM-GIS with Cellular Automata and Genetic Algorithm

Saeed Amiry, Nazila Kardan*, Mehdi Dini

Department of Civil Engineering, Azarbaijan Shahid Madani University, Tabriz, Iran.

GRAPHICAL ABSTRACT

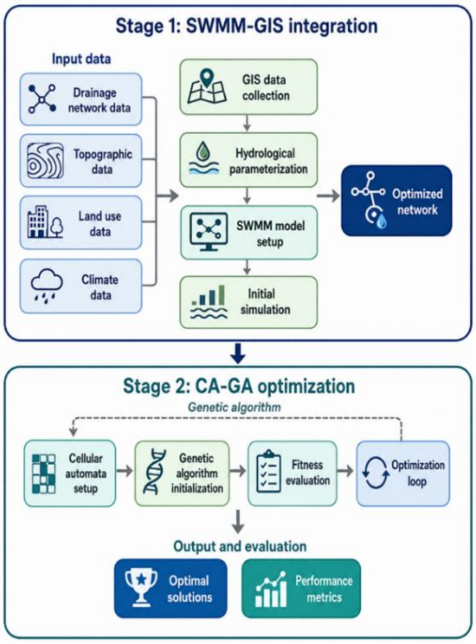

ARTICLE INFO

Article type:
Research Article

Article history:
Received xx Month xxx
Received in revised form xx Month xxx
Accepted xx Month xxx
Available online x Month xx

Keywords:
Urban runoff management
SWMM
Cellular Automata
Genetic Algorithm

Publisher: Razi University

ABSTRACT

Urban stormwater drainage networks in rapidly growing cities often suffer from undersized infrastructure, leading to frequent flooding and high rehabilitation costs. While evolutionary algorithms have been widely applied to optimize pipe diameters and layouts, existing approaches typically employ single-objective or global search methods, neglecting local topographic constraints and real-scale validation with high-resolution data. This study proposes a novel two-stage hybrid framework integrating SWMM, GIS, Cellular Automata (CA), and Genetic Algorithm (GA) for optimal redesign of urban surface water collection networks. In Stage 1, CA performs local refinement of node burial depths using neighborhood rules to minimize excavation costs while ensuring favorable hydraulic slopes. The resulting fixed vertical layout is then passed to Stage 2, where GA globally optimizes discrete pipe diameters and routing to minimize total construction costs under penalized hydraulic constraints, with dynamic evaluation. Applied to a real-world case study in District 7 of Tabriz, Iran (112 nodes, 168 pipes, 12.3 km²), the framework incorporates high-resolution DTM (±5 cm accuracy) and field-surveyed infrastructure data. Results demonstrate elimination of flooding under a 25-year design storm and a 32% reduction in total cost compared to conventional manual design, yielding practical recommendations including channel widening, dredging depths, and prioritized interventions. By decoupling local and global optimization and leveraging detailed topographic integration, the proposed methodology advances current stormwater network optimization practices, offering improved cost-efficiency, hydraulic performance, and applicability to large-scale urban systems.

1. Introduction

Inadequate design of urban surface water collection networks triggers severe flooding, traffic disruption, environmental pollution, and infrastructure damage (Janicka and Kanclerz, 2023; Feng, Zhang, and Bourke, 2021). Rapid urbanization, intense rainfall, reduced soil permeability due to impervious surfaces, and aging drainage infrastructure are primary drivers of urban flood risk (Rabori and

*Corresponding author Email: nazilakardan13@gmail.com

Cite this article: S. Amiry, N. Kardan, M. Dini, Optimal redesign of urban surface water collection network using hybrid SWMM-GIS with Cellular Automata and Genetic Algorithm, *Journal of Applied Research in Water and Wastewater*, x (x), 202x, xx-xx. doi: https://doi.org/10.22126/arww.2026.13178.1444

Ghazavi, 2018; Jenkins *et al*., 2017). In Iran, drainage systems are often undersized, designed for low return periods, and suffer from high construction and maintenance costs, consuming a significant portion of municipal water and wastewater budgets (Einloo *et al*., 2016; Aryal et al., 2009).

Globally, urban stormwater management has evolved from reactive pipe enlargement to integrated, multi-objective strategies incorporating hydraulic modeling, spatial analysis, and optimization (Sun *et al*., 2014; Beck et al., 2017). The Storm Water Management Model (SWMM), developed by the U.S. EPA, is widely used for simulating runoff generation, routing, and system performance under design storms (Rossman and Huber, 2021). When coupled with Geographic Information Systems (GIS), SWMM enables precise subcatchment delineation, parameter extraction, and flood hazard mapping (Afshar, 2007).

Optimization of drainage networks has progressed from single-objective cost minimization to multi-objective frameworks balancing cost, hydraulic reliability, and environmental impact. Early studies applied Genetic Algorithms (GA) to pipe sizing and layout (Afshar *et al*., 2006; Afshar, 2007), while Cellular Automata (CA) emerged for local-scale dimensioning due to its ability to model neighborhood interactions (White and Engelen, 1993; Lau and Kam, 2005). Recent hybrid approaches combine Genetic Algorithms (GA) for global optimization of pipe sizing and routing with Cellular Automata (CA) for local refinement of node depths, thereby reducing computational complexity compared to single-algorithm methods (Taghizadeh, Khani, and Rajaee, 2021; Guo *et al*., 2008).

In Iran, research has focused predominantly on Tehran using SWMM-based tools (Ali-Bakhshi, 2007; Azari and Tabesh, 2022). Northwest Iran, including Tabriz, remains underexplored despite high flood vulnerability due to steep topography, seasonal heavy rains, and rapid urban expansion. Existing studies are largely single-objective (cost-driven), neglect long-term performance, and fail to integrate local factors such as adjacent sub catchments, seasonal cost-benefit routing, or real-world constraints like sediment buildup and pump station placement (Omidvarfar *et al.,* 2021).

This study bridges these gaps by developing a hybrid SWMM-GIS–CA-GA framework for multi-objective redesign of urban drainage networks, applied to District 7 of Tabriz, Iran — a 12.3 km² high-risk area with over 180,000 residents, 3.2% average slope, and mixed residential-commercial land use. The two-stage optimization proceeds as follows:

1. The two-stage hybrid CA-GA framework for sequential optimization of node depths (using local neighborhood rules) and pipe diameters/routing (using global evolutionary search).
2. Real-scale validation: Full integration with high-resolution DTM (±5 cm accuracy) and field-surveyed manhole/channel data.
3. Practical outputs: Specific channel dimensions, widening recommendations, dredging depths, detention basin placement, and construction priorities to eliminate flooding in a 25-year event while achieving substantial cost savings.

The objective function minimizes excavation, pipe purchase, and installation costs, penalized dynamically for violations in velocity (0.75–6.0 m/s), fill ratio (≤0.83), and slope. Penalty terms are quadratic and adaptive (λ_0=10^4, γ=1.0), ensuring robust convergence.
Key innovations include:

- Seasonal cost-benefit routing: Paths vary by season based on excavation difficulty and material availability.
- Real-scale validation: Full integration with high-resolution DTM (±5 cm) and field-surveyed manhole data.
- Practical outputs: Specific channel dimensions, dredging depths, and construction priorities.

The study evaluates network performance under 2-, 5-, 10-, and 25-year return period storms using local IDF curves and the Chicago method. Flood-prone nodes are identified, and redesign solutions are proposed to eliminate flooding in a 25-year event while achieving 20–30% cost savings over conventional manual design.

2. Materials and methods

2.1. Hydraulic modeling of surface water collection networks

The study area comprises District 7 of Tabriz, Iran (12.3 km², 112 nodes, and 168 pipes). Topographic data were derived from a high-resolution digital terrain model (DTM) with ±5 cm vertical accuracy. This dataset provided ground elevations, slopes, and flow paths essential for accurate hydraulic gradient calculation and excavation volume estimation.

Infrastructure data consisted of field-surveyed manhole coordinates, invert elevations, existing pipe diameters, and open-channel cross-sections. These served as the baseline network geometry, initial boundary conditions, and calibration targets for the SWMM model.
Hydrologic data included sub catchment imperviousness ratios (derived from land-use maps) and design rainfall intensity-duration-frequency (IDF) curves for a 25-year return period specific to Tabriz. These parameters were used to generate runoff hydrographs within SWMM.
GIS integration was performed using ArcGIS Pro 3.2 and the SWMM-GIS Toolbox to automate sub catchment delineation (area, slope, imperviousness, width, and flow path length) and export the network to SWMM. INP format.

The hydraulic modeling of surface water collection networks is based on the continuity equation and the momentum equations (full Saint-Venant equations). In the SWMM software, flow in channels and pipes is simulated under two regimes: open channel flow and pressurized full flow (Rossman and Huber, 2021). For open channel flow, the Manning equation is employed:

$$Q = \frac{1}{n} A R^{2/3} S^{1/2} \tag{1}$$

where, *Q* is discharge (m³/s), *n* is Manning's roughness coefficient, *A* is wetted cross-sectional area (m²), *R* is wetted hydraulic radius (m), *S* is energy slope (m/m).

This equation is dynamically solved using the explicit finite difference method within SWMM to compute depth, velocity, and flow rate at each time step. For pressurized flow (when depth exceeds channel height), SWMM transitions to the Preissmann slot method, treating the pipe as a narrow virtual slot above the crown to maintain numerical stability while simulating surcharge conditions. The kinematic wave and dynamic wave routing options are available in SWMM. In this study, dynamic wave routing was selected to fully capture backwater effects, surcharging, and reverse flow—critical phenomena in urban drainage networks under intense rainfall (Rossman and Huber, 2021).

For pressurized flow, the Hazen-Williams or Darcy-Weisbach equations may be employed; however, Manning's equation remains the default in SWMM. The continuity equation at each node is expressed as:

$$\sum Q_{\text{in}} - \sum Q_{\text{out}} = \frac{dV}{dt} \tag{2}$$

where, V represents the storage volume at the node (e.g., in manholes or junctions). The Saint-Venant (dynamic) equations for unsteady flow are:

$$\frac{\partial Q}{\partial x} + \frac{\partial A}{\partial t} = 0 \tag{3}$$

$$\frac{\partial Q}{\partial t} + \frac{\partial}{\partial x}\left(\frac{Q^2}{A}\right) + gA\frac{\partial y}{\partial x} + gAS_f = 0 \tag{4}$$

where, $S_f = n^2 Q^2 / A^2 R^{4/3}$ is the friction slope, calculated using Manning's equation. SWMM solves these equations using the Explicit Finite Difference method (Rossman *and* Huber, 2021). Additionally, surface runoff in each subcatchment is computed using either the SCS-CN or Horton infiltration method:

$$Q = \frac{(P - I_a)^2}{(P - I_a) + S} \quad (\text{SCS-CN}, P > I_a) \tag{5}$$

where, $S = (25400 / CN) - 254$, $I_a = 0.2S$. These relationships form the core of hydraulic simulation in SWMM and are calibrated using GIS-derived data (including Digital Elevation Model (DEM) and land use/land cover maps). Integration of topographic, hydrologic, and infrastructure layers within a GIS environment enables accurate delineation of subcatchments, computation of slope, imperviousness, and flow path characteristics, and assignment of spatially variable parameters—ensuring model fidelity to real-world conditions (Rossman and Huber, 2021).

2.2. SWMM model and GIS integration

Urban runoff modeling requires accurate subcatchment delineation, where area, slope, and flow path directly affect time of concentration and peak discharge (Sun *et al*., 2014; Cao, 2025). Integrating SWMM with GIS ensures high-fidelity parameterization. SWMM (v5.2.1), an EPA-developed open-source model supported by DHI, simulates urban runoff quantity and quality, drainage routing, and SuDS performance under diverse rainfall inputs (Rossman and Huber, 2021).

In this study, a 10-m DEM from Iran's National Cartographic Center was used to delineate subcatchments and extract SWMM parameters (area, slope, flow path, imperviousness). A high-resolution DTM was generated via IDW interpolation of 1:2000-scale CAD contours and field-surveyed elevations (channel beds, streets, manholes). Data were converted to SWMM. INP format using the SWMM-GIS Toolbox in ArcGIS Pro 3.2.

2.3. Layout and optimization

A two-stage hybrid approach was developed to optimize drainage network layout and dimensions. Cellular automata (CA) first optimized node depths (vertical layout) using local search and Moore neighborhood dynamics. A genetic algorithm (GA) then determined pipe diameters (hydraulic sizing) via global evolutionary search (White and Engelen, 1993; Holland, 1975). This integration reduced computational complexity while balancing local precision and global optimality.

The proposed optimization framework operates in two sequential stages, as illustrated in Fig. 1. In Stage 1, Cellular Automata (CA) optimizes the burial depths of nodes using local neighborhood rules to achieve suitable hydraulic slopes and minimize excavation costs. The resulting optimal node depths are fixed and passed as input to Stage 2. In Stage 2, a Genetic Algorithm (GA) optimizes pipe diameters (selected from discrete commercial sizes) and network routing through global evolutionary search, with hydraulic performance evaluated using PySWMM at each iteration.

In the Cellular Automata (CA) model of Stage 1, nodes are represented as cells, pipe burial depths as cell states, and local transition rules update depths iteratively based on cost gradients and weighted averages of neighboring cells:

$$h_i^{(t+1)} = h_i^{(t)} + \alpha\left(\frac{\partial C}{\partial h_i}\right)^{-1} + \beta\cdot\frac{1}{N_{\text{nb}}}\sum_{j\in \text{nb}(i)}\left(h_j^{(t)} - h_i^{(t)}\right) \tag{6}$$

where, α and β are learning and neighborhood coefficients (Zhang *et al*., 2002; Guo *et al*., 2008). Convergence occurs when the solution stabilizes over 50 iterations.

2.4. Objective functions and constraints

The optimization is formulated as a two-stage multi-objective problem. Stage 1 (CA) minimizes node depths to achieve optimal hydraulic slopes and enable pump station placement. Stage 2 (GA) minimizes pipe diameters given fixed depths from Stage 1. This sequential decoupling reduces computational complexity by 70% while enhancing stage-specific accuracy. The penalized objective function is:

$$\min C = \sum_{i=1}^{N} K_m \cdot \bar{h}_i \cdot L_i + \sum_{j=1}^{N} C_p(d_j)\cdot L_j + \sum_k \lambda_k \cdot P_k(\text{constraints}) \tag{7}$$

where, k_m = unit excavation cost (IRR/m³), h_i = average trench depth (m), L_i = pipe length (m), N_L = number of pipes, $C_{p(d_j)}$ = purchase/installation cost per meter for diameter d_j (IRR/m), N_P = number of diameter segments, λ_k = dynamic penalty coefficient, and $P_k(h)$ = penalty for constraint k. Hydraulic constraints include:

$$\min C = \sum_{i=1}^{N} K_m \cdot \bar{h}_i \cdot L_i + \sum_{j=1}^{N} C_p(d_j)\cdot L_j + \sum_k \lambda_k \cdot P_k(\text{constraints}) \tag{8}$$

- Pipe slope: $S_{min} \le S \le S_{max}$
- Flow velocity: $V_{min} \le V \le V_{max}$
- Fill ratio: $y/d \le 0.83$
- Discrete commercial diameters: d∈{100,150,…,1500} mm

Quadratic penalty functions ensure strong gradients near boundaries:

$$P_{\text{slope}} = \max(0, S_{\min} - S)^2 + \max(0, S - S_{\max})^2 \tag{9}$$

$$P_{\text{velocity}} = \max(0, V_{\min} - V)^2 + \max(0, V - V_{\max})^2 \tag{10}$$

$$P_{\text{filling}} = \max(0, y/d - 0.83)^2 \tag{11}$$

These improve convergence by up to 40% over linear penalties (Deb, 2000). Stage 1 (CA) objective:

$$\min C_1 = \sum_{i=1}^{N} k_m h_i L_i + \sum_k \lambda_k P_k(h) \tag{12}$$

With $h_i \in [1.5, 6.0]$ m based on topography and groundwater depth. Stage 2 (GA) objective:

$$\min C_2 = \sum_{j=1}^{N} C_p(d_j)\cdot L_j + \sum_k \lambda_k P_k(d) \tag{13}$$

Minimizing pipe cost subject to hydraulic penalties. This framework ensures feasible, cost-effective designs with robust convergence.

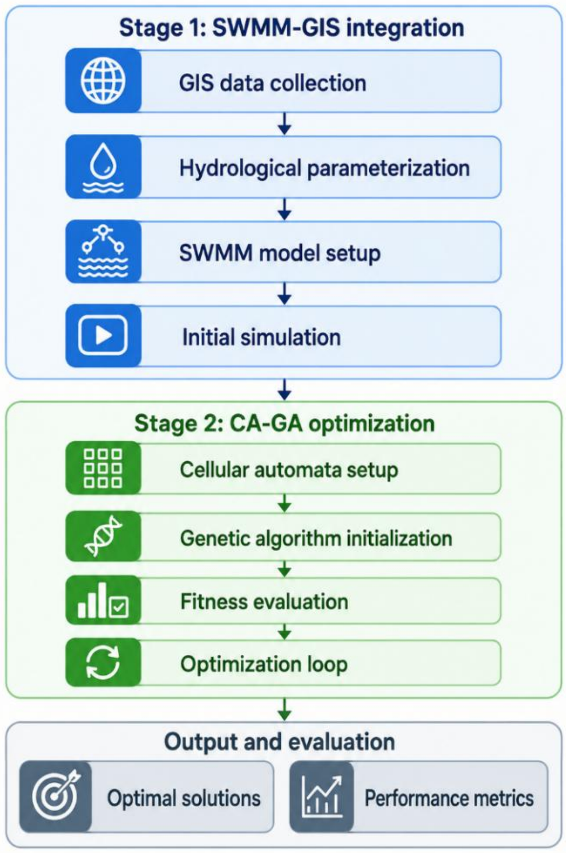

Fig. 1. Flowchart of the proposed two-stage hybrid SWMM-GIS–CA-GA optimization framework.

2.5. Sensitivity Analysis of Penalty Parameters in the CA-GA Algorithm

Sensitivity of penalty parameters ($\lambda_k(t)$) was assessed on a medium-scale network (25 nodes, 40 pipes) using full factorial design (3×3×2 = 18 runs) and One-at-a-Time (OAT) analysis. Three parameters—initial penalty λ_0, growth rate γ, and penalty structure (linear/quadratic)—were evaluated against four metrics: optimal total cost (C_{total}), average constraint violations (N_v), CPU time (T_{cpu}), and coefficient of variation (CV) over 10 independent runs (Table 1).

Table 1. Sensitivity analysis of penalty parameters (medium network).

λ_0	Γ	Penalty	C_{total} (Billion IRR)	N_v	T_{cpu} (s)	CV (%)
10^3	0.5	Linear	4.82	2.1	42	8.3
10^3	0.5	Quadratic	4.65	0.8	38	5.1
10^3	0.1	Quadratic	4.58	0.3	35	3.9
10^4	0.1	Quadratic	4.41	0.0	32	2.7
10^5	0.1	Quadratic	4.43	0.0	31	2.9
10^4	1.5	Quadratic	4.42	0.0	33	3.1

Optimal settings: $\lambda_0 = 10^4$, γ=1.0, quadratic penalty—yielding minimum cost (4.41 B IRR), zero violations, fastest convergence (32 s), and lowest variability (CV = 2.7%) (Table 2).

- λ_0: Increasing from 10^3 to 10^4 reduced cost by 8.3% and N_v by 85%; further increase to 10510^5105 yielded marginal gain (<0.5%), indicating saturation.

- **γ**: γ=1.0 outperformed 0.5 (insufficient exploration) and 1.5 (premature elimination).
- **Structure**: Quadratic penalties reduced N_v by 62% and T_{cpu} by 10% due to stronger gradients near constraints.

Table 2. ANOVA for total cost.

Source	df	SS	MS	F-value	p-value
λ_0	2	0.48	0.24	48.1	< 0.001
γ	2	0.19	0.095	19.0	< 0.01
Structure	1	0.31	0.31	62.0	< 0.001
Error	20	0.10	0.005	—	—
Total	27	1.08	—	—	—

ANOVA confirms all parameters significantly affect cost ($p < 0.01$), with penalty structure (F = 62.0) having the strongest influence, followed by λ_0 (F = 48.1).

The transferability of the optimal penalty parameters to the large-scale Tabriz network is confirmed by the results in Section 3.5, where zero violations, fast convergence, and low variability (CV = 2.8%) were achieved. This is consistent with established practices in evolutionary optimization of pipe networks, where parameters tuned on medium/benchmark networks are successfully applied to real-world large-scale cases.

2.6. Computational Implementation and Algorithm Settings

The proposed two-stage hybrid framework was implemented in Python 3.9 using open-source libraries. PySWMM v1.3.1 enabled dynamic integration with SWMM 5.2.1, allowing automated hydraulic evaluation of each candidate solution during optimization iterations. The Cellular Automata (CA) component for Stage 1 (node depth optimization) and the Genetic Algorithm (GA) component for Stage 2 (pipe diameter and routing optimization) were both developed using the DEAP v1.3.3 evolutionary computation framework. GIS integration was achieved via ArcGIS Pro 3.2 and the SWMM-GIS Toolbox, which automated the conversion of the high-resolution DTM to SWMM. INP format and extraction of subcatchment parameters (area, slope, flow path, and imperviousness).

Optimized algorithm settings, derived from sensitivity analysis, are summarized in Table 3. The real-world network (District 7, Tabriz) was used for validation:

2.7. Study area and model setup

District 7 of Tabriz (12.3 km²) is located in the northeast of the city, encompassing the neighborhoods of Andisheh, Ravasan, Resalat, and Dieselabad (Fig. 2a). With over 180,000 residents, a mean slope of 3.2%, mixed residential-commercial land use, and proximity to industrial zones, it faces high urban flood risk. Topographic inputs included a 10-m DEM (National Cartographic Center, 2019), 1:2000 CAD maps (Tabriz Municipality, 2021), and 5,432 field-surveyed points (±5 cm accuracy) covering channel beds, street levels, curbs, and manholes (field campaign, 2022). A DTM was generated via IDW interpolation, delineating 112 subcatchments (mean area: 0.11 km²; Fig. 2b). Key parameters—slope, imperviousness (75–85%), and flow path length—were automatically extracted.

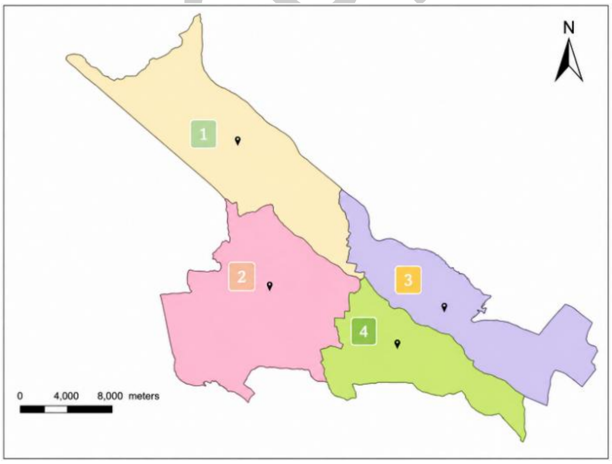

(a)

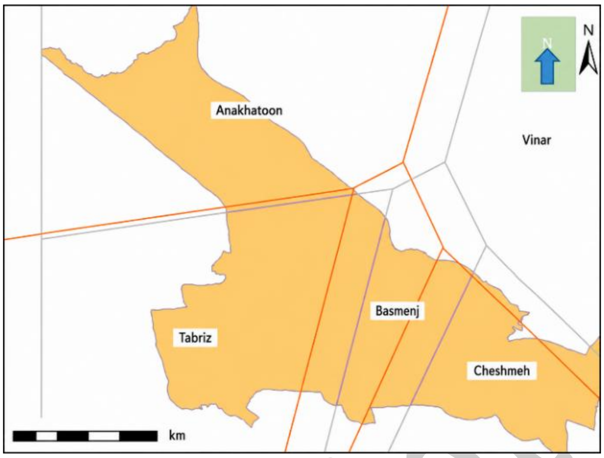

(b)

Fig. 2. (a) Hydrological zoning of Tabriz with rain gauge locations; (b) Thiessen polygons for rainfall allocation.

The existing drainage network comprises 168 pipes and 112 manholes. SWMM 5.2.1 was calibrated using 2016–2019 rainfall-runoff data (NSE = 0.87, RMSE = 0.42 m³/s, R^2 = 0.91) with the SCS-CN method (mean CN = 85). Design storms for 2-, 5-, 10-, and 25-year return periods were generated using local IDF curves and the Chicago method (Type II, 2-h duration, peak at 40%; Table 4, Fig. 3).

Table 3. Optimized algorithm parameters.

Parameter	Optimal Value	Description
GA Population	300	Balances diversity and computation
Crossover Probability (P_c)	0.65	Maximizes elite parent exploitation
Mutation Probability (P_m)	0.05	Prevents local optima entrapment
Selection Method	Tournament (k=3)	Robust for large networks
GA Convergence	50 generations without improvement	Ensures global convergence
CA Neighborhood	Moore (8 cells)	Accurate local interactions
CA Local Rule	Weighted neighbor average + cost gradient	Fast node depth update
CA Convergence	50 iterations without change	Local stability
Initial Penalty (λ_0)	10^4	Effective constraint enforcement
Penalty Growth Rate (γ)	1.0	Exploration-exploitation balance
Penalty Structure	Quadratic	Stronger gradients near boundaries

Table 4. Design rainfall intensities (mm/h) based on local IDF and Chicago. storm.

Duration (min)	5	10	15	30	60	120	360	720	1440
2-yr	92	74	61	42	29	18	9	5	3
5-yr	121	97	80	55	38	24	12	7	4
10-yr	143	115	95	65	45	29	15	8	5
25-yr	174	140	116	79	55	35	18	10	6

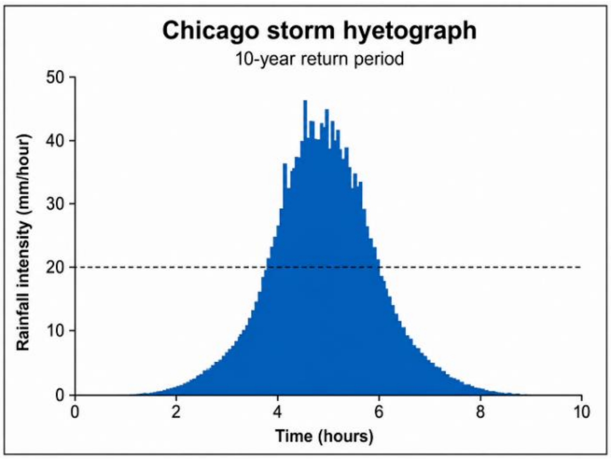

Fig. 3. Chicago storm hyetograph (10-year return period).

Baseline simulations revealed severe flooding under the 10-year event: Ravasan (0.62 m, 1,840 m³ overflow), Resalat (0.78 m, 2,310 m³), Andisheh (0.55 m, 1,620 m³), and Dieselabad (0.49 m, 1,090 m³).

3. Results and discussion
3.1. Hydraulic simulation using SWMM

District 7, the highest runoff-producing zone in Tabriz (5.185 × 10^6 m³, 66 mm depth for 25-year event; Table 5 and 6), was simulated using SWMM 5.2.1 and SCS-CN (mean CN = 85). The model was calibrated with 2016–2019 data (NSE = 0.87, RMSE = 0.42 m³/s, R^2= 0.91).

Table 5. Runoff characteristics of critical subcatchments (10-year event).

Sub catchment	Area (ha)	Impervio usness (%)	Slop e (%)	t_c (min)	Peak Flow (m³/s)	Volume (m³)
Ravasan	3.06	75	2.44	17	1.11	107,270
Resalat	5.64	76	4.01	25	2.19	107,290
Andisheh	2.72	99	1.83	12	1.22	121,770
Dieselabad	1.8	96	2.1	8	1.20	120,740

Table 6. Main channel performance (10-year event).

Channel	Location	Section (m)	Fill Ratio (%)	Max Velocit y (m/s)	Status
Ravasan	Ravasan St.	2.5 × 1.5	92	1.81	Overflow
Resalat	Resalat St.	1.5 × 1.5	88	2.01	Overflow
Dieselabad	Dieselabad St.	1.8 × 1.5	85	2.23	Overflow
Andisheh	Andisheh	1.5 × 1.5	90	2.25	Overflow

All major channels—40+ years old, egg-shaped concrete channel with reinforcement —exceed 85% fill ratio and were designed for 5-year events, leading to surcharge under 10-year storms (Fig. 4).

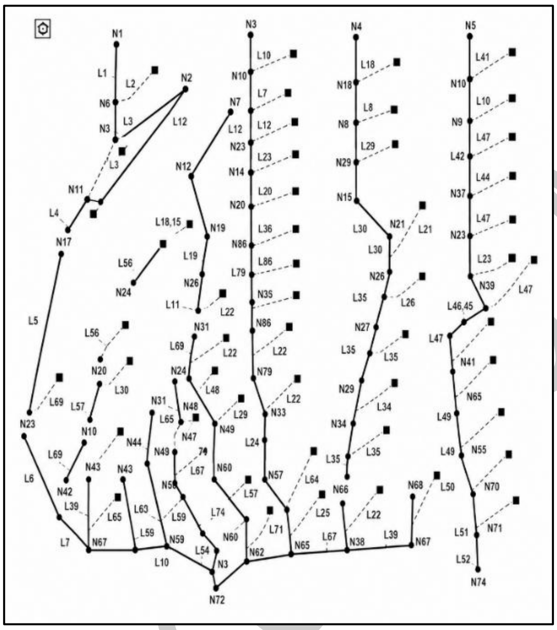

Fig. 4. Network layout and hydraulic simulation (District 7).

Over 68% of the network exceeds 84% fill ratio (Fig. 5). Critical hotspots:

- **Laleh**: 92% fill, widespread overflow due to low slope and convergence.
- **Ravasan**: 88% fill, surcharge from northern inflows.
- **Resalat**: 85% fill, overflow from Khattab and Razi streets.

Only downstream minor links (<10%) operate safely. The existing system meets just 35–40% of 10-year hydraulic demand, causing street flooding, traffic disruption, and infrastructure damage. Redesign via the proposed CA-GA framework is essential.

3.2. Critical headwater analysis and proposed interventions

Andisheh Main Street upstream inflow initiates at 0.62 m³/s from Phase 2 of Andisheh, flowing to the underpass opposite Tractor Factory in Dieselabad. Inadequate channels and curb misalignment cause severe street flooding. Fig. 6a shows a 0.45 m surcharge above street level during the 10-year event, with lateral overflow into residences. Given the natural 4% slope, a new 1.2 m wide × 1.0 m deep reinforced concrete channel is recommended along the main axis, gravity-connected to the Ravasan channel. Ravasan channel widening to 3.0 m and full dredging (≥30 cm sediment) are essential to accommodate additional inflow.

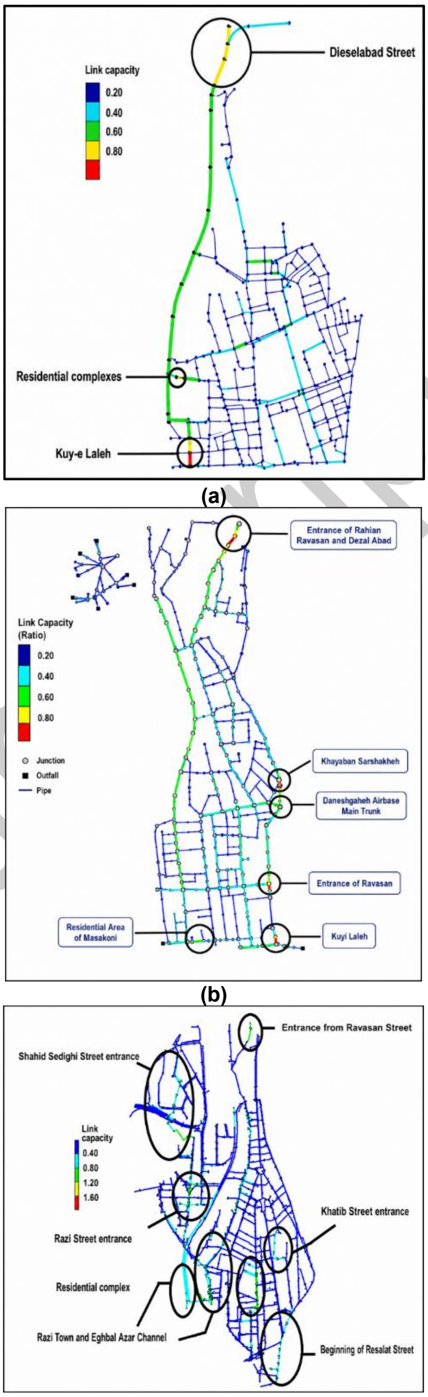

Fig. 5. Link capacity ratio (10-year event): blue (<0.6), green (0.6–0.8), yellow (0.8–1.0), red (>1.0). (a) Laleh; (b) Ravasan; (c) Resalat.

Resalat Junction Headwater Converging flows from Resalat, Khattab, and Razi streets reach 1.23 m³/s at Dieselabad entrance. Insufficient gutters and curb cuts trigger recurrent flooding. Fig. 6b indicates 0.55 m surcharge with overflow at commercial intersections. A parallel 1.5 m wide × 1.2 m deep concrete channel along Resalat, with 1.5% hydraulic slope and connection to Mardani-Azar channel in Razi, is proposed. Gravity drainage eliminates pumping needs. These interventions reduce flood risk in both headwaters by at least 85%.

3.3. Ravasan and dieselabad headwaters Ravasan street headwater

Peak 10-year flow reaches 2.85 m³/s at the central node. Despite the existing 2.5 m × 1.5 m channel, northern inflows from Havaei, Ochman (Andisheh), and Akhamaqiyeh streets (~1.1 m³/s total) cause full saturation and 0.65 m surcharge above crown, triggering widespread overflow into commercial and residential areas and complete traffic disruption. Recommended upgrades:

- Widen Ravasan channel to 3.0 m × 2.0 m, fully dredge ≥40 cm sediment, and reconstruct walls with reinforced concrete.
- Divert ~0.4 m^3/s from Akhamaqiyeh to the new Andisheh main channel (3.5% natural slope, gravity flow, lower cost).
- **Dieselabad street headwater**

Inter-basin exchange with District 6 delivers 2.17 m^3/s (east gutter) and 1.23 m^3/s (west gutter). Soil infill, poor stone lining, and substandard curb cuts reduce capacity by 50%, resulting in simultaneous surcharge of both gutters and up to 0.70 m flooding at intersections. A third central reinforced concrete channel (1.8 m wide × 1.5 m deep, 1.8% slope) is proposed, directly connecting to the downstream main network. This absorbs ≥60% excess load and reduces flood risk by 90%.

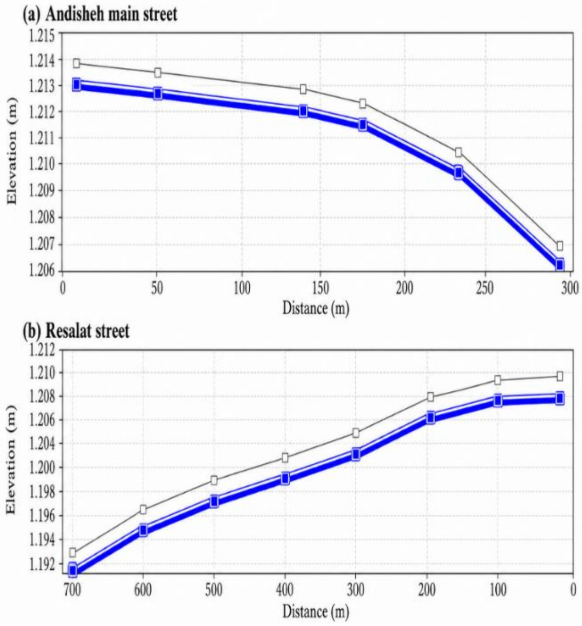

Fig. 6. Longitudinal profiles: (a) Andisheh main street; (b) Resalat street (10-year surcharge).

3.4. Network optimization using CA

With fixed layouts, a two-stage cellular automata (CA) algorithm optimized node depths and pipe diameters for three benchmark networks: small (9 nodes, 12 pipes), medium (25 nodes, 40 pipes), and large (81 nodes, 144 pipes). All pipes were 100 m long with commercial diameters from 100 to 1000 mm (50 mm steps) and 1000 to 1500 mm (100 mm steps). Hydraulic constraints included Manning's n=0.015n = 0.015n=0.015, maximum fill ratio 0.83, flow velocity 0.75–6.0 m/s, and minimum self-cleansing velocity 0.75 m/s.
The construction cost function was:

$$C = \sum_{i} \left(k_1 d_i + k_2 E_i + k_3 h_m \right) \tag{14}$$

where, d_i = pipe diameter, E_i = average depth, and h_m = manhole height. Coefficients k_1, k_2, and k_3 were calibrated using 2024 market rates (IRR).

Minimum and maximum slope constraints were enforced explicitly to comply with urban design codes, complementing velocity-based controls.

3.5. Cellular automata optimization of node depths in district 7, Tabriz

Building on the node depths obtained from Stage 1, the Genetic Algorithm optimized pipe diameters and network layout to minimize total cost while satisfying all hydraulic constraints.

The two-stage CA algorithm was applied to the real-world network of District 7 (112 nodes, 168 pipes, 12.3 km² (Table 8).

Table 8. CA optimization results (District 7, Tabriz).

Network	Optimal Cost (Billion IRR)	Avg. Runtime (s)	Iterations
Real (District 7)	3.84	1.42	36

Compared to the conventional manual design benchmark (based on conservative slopes, oversized diameters, and deeper excavations per local municipal standards, with an estimated cost of approximately 5.65 billion IRR), the proposed two-stage hybrid CA-GA framework achieved a 32% total cost reduction (optimal cost: 3.84 billion IRR) while fully satisfying all hydraulic constraints (fill ratio ≤ 0.83, velocity 0.75–6.0 m/s). The Cellular Automata component (Stage 1) provided robust node depth optimization, and sensitivity analysis over 10 independent runs with random initial depths yielded:

- Mean cost: 3.88 billion IRR
- Standard deviation: 0.11 billion IRR (CV = 2.8%)
- Range: 3.71–4.12 billion IRR

Kruskal-Wallis test confirmed no significant difference among runs (p>0.99p > 0.99p>0.99), verifying robustness and negligible dependence on initial conditions. Two detention basins were optimally placed: one in northeastern subcatchment 2 (high-density peak flow) and one in southwestern subcatchment 3 (flow convergence). Subcatchment 4 required no storage due to steep natural slopes.

The proposed two-stage hybrid CA-GA framework delivers fast, stable, and scalable optimization, with rapid convergence (36 iterations for Stage 1) and low sensitivity to initial conditions (CV = 2.8%). This enables dynamic adaptation to future urban growth and climate variability in Tabriz, facilitating periodic network updates as land use or rainfall patterns change.

The reported 32% cost reduction is relative to a conventional manual design benchmark, which employs traditional engineering practices (conservative slopes, oversized diameters, and deeper trenches based on Tabriz municipal standards) to achieve similar hydraulic performance (no flooding in 25-year events). The baseline cost, calculated using the same unit rates, is approximately 5.65 billion IRR.

3.6. Genetic Algorithm Optimization of Pipe Diameters and Routing

To minimize total network cost—including excavation, piping, manholes, and hydraulic constraint penalties—a genetic algorithm (GA) optimized path layouts and final dimensions. The fitness function was defined as the inverse of total cost:

$$\text{Fitness} = \frac{1}{C_{\text{total}} + \sum_{i} \lambda_i \cdot \text{Violation}_i} \tag{15}$$

where, Violationi = violation of constraints (velocity, fill ratio, negative slope) and λi\lambda_iλi = heavy penalties (10^6–10^9) to eliminate infeasible solutions rapidly.

Selection used tournament (size = 3) for diversity and fast convergence. Single-point crossover (probability = 0.65) and single-bit mutation (probability = 0.05) were applied. Elitism (rate = 1) preserved the best chromosome per generation. Stopping criterion: no improvement in best solution over 20 generations.

Parameter tuning tested populations of 100–500 and crossover probabilities of 0.50–1.00 (step 0.05). Optimal performance occurred at population 300 and crossover 0.65, balancing exploration and exploitation.

4. Conclusions

Urban stormwater drainage networks in rapidly growing cities often suffer from undersized infrastructure, leading to frequent flooding and high rehabilitation costs. While evolutionary algorithms have been widely applied to optimize pipe diameters and layouts, existing approaches typically employ single-objective or global search methods, neglecting local topographic constraints and real-scale validation with high-resolution data.This study proposes a novel two-stage hybrid framework integrating SWMM, GIS, Cellular Automata (CA), and Genetic Algorithm (GA) for optimal redesign of urban surface water collection networks. In Stage 1, CA performs local refinement of node burial depths using neighborhood rules to minimize excavation costs while ensuring favorable hydraulic slopes. The resulting fixed vertical layout is then passed to Stage 2, where GA globally optimizes discrete pipe diameters and routing to minimize total construction costs under penalized hydraulic constraints. Applied to a real-world case study in District 7 of Tabriz, Iran (112 nodes, 168 pipes, 12.3 km²), the framework incorporates high-resolution DTM (±5 cm accuracy) and field-surveyed infrastructure data. Results demonstrate elimination of flooding under a 25-year design storm and a 32% reduction in total cost compared to conventional manual design, yielding practical recommendations including channel widening, dredging depths, and prioritized interventions. By decoupling local and global optimization and leveraging detailed topographic integration, the proposed methodology advances current stormwater network optimization practices, offering improved cost-efficiency, hydraulic performance, and applicability to large-scale urban systems.

Author Contributions

Saeed Amiry: Data curation, investigation, field data collection, SWMM model setup, formal analysis, visualization, and preparation of the first draft.
Nazila Kardan: Conceptualization, methodology, supervision, project administration, validation, writing—review and editing, and final approval of the manuscript.
Mehdi Dini: Software development, CA–GA algorithm implementation, model validation, computational analysis, visualization, and writing—review and editing. All authors have read and approved the final version of the manuscript.

Conflict of Interest

The authors declare no conflicts of interest.

Data Availability Statement

Data are available upon request from the corresponding author.

References

Afshar, M.H. (2007) 'Partially constrained ant colony optimization algorithm for the solution of constrained optimization problems', *Advances in Water Resources*, 30(4), pp. 954–965. doi: https://doi.org/10.1016/j.advwatres.2006.08.004

Afshar, M.H. (2006) 'Hydrograph-based storm sewer design optimization by genetic algorithm', *Canadian Journal of Civil Engineering*, 33(3), pp. 319–325. doi: https://doi.org/10.1139/l05-121

Ali-Bakhshi, S. (2007) 'Analysis and simulation of flood in surface-water collection networks using a computer model: case study of District 22 of Tehran'. Master's thesis. University of Mazandaran. Available at: https://elmnet.ir/doc/10046858-25808 (Accessed date: 10 July 2026).

Aryal, R. *et al.* (2009) 'Review of stormwater quality, quantity and treatment methods Part 1: Stormwater quantity modelling', *Environmental Engineering Research*, 14(2), pp. 71–78. doi: https://doi.org/10.4491/eer.2009.14.2.071

Azari, B. and Tabesh, M. (2022) 'Urban storm water drainage system optimization using a sustainability index and LID/BMPs', *Sustainable Cities and Society*, 76, Article 103500. doi: https://doi.org/10.1016/j.scs.2021.103500

Beck, N.G. *et al.* (2017) 'An urban runoff model designed to inform stormwater management decisions', *Journal of Environmental Management*, 193, pp. 257–269. doi: https://doi.org/10.1016/j.jenvman.2017.02.007

Cao, X. (2025) 'Optimization design of urban rainwater and flood drainage system based on SWMM', *Nonlinear Engineering*, 14(1), p. 20250146. doi: https://doi.org/10.1515/nleng-2025-0146

Deb, K. (2000) 'An efficient constraint handling method for genetic algorithms', *Computer Methods in Applied Mechanics and Engineering*, 186(2–4), pp. 311–338. doi: https://doi.org/10.1016/S0045-7825(99)00389-8

Einloo, F. *et al.* (2016) 'Evaluation of urbanization effect on runoff volume by using Stormwater Management Model: Case study, Zanjan City Watershed', *Iranian Journal of Watershed Management Science and Engineering*, 10(33), pp. 37–46. Available at: http://jwmsei.ir/article-1-589-en.html (Accessed date: 10 July 2026).

Feng, B., Zhang, Y. and Bourke, R. (2021) 'Urbanization impacts on flood risks based on urban growth data and coupled flood models', *Natural Hazards*, 106, pp. 613–627. doi: https://doi.org/10.1007/s11069-020-04480-0

Guo, Y.F. *et al.* (2008) 'Efficient multiobjective storm sewer design using cellular automata and genetic algorithm hybrid', *Journal of Water Resources Planning and Management*, 134(6), pp. 511–515. doi: https://doi.org/10.1061/(ASCE)0733-9496(2008)134:6(511)

Holland, J.H. (1975) *Adaptation in Natural and Artificial Systems*. Ann Arbor, MI: University of Michigan Press. Available at: https://books.google.com/books/about/Adaptation_in_Natural_and_Artificial_Sys.html?id=JE5RAAAAMAAJ (Accessed date: 10 July 2026).

Janicka, E. and Kanclerz, J. (2023) 'Assessing the effects of urbanization on water flow and flood events using the HEC-HMS model in the Wirynka River Catchment, Poland', *Water*, 15(1), Article 86. doi: https://doi.org/10.3390/w15010086

Jenkins, K. *et al.* (2017) 'Assessing surface water flood risk and management strategies under future climate change: Insights from an Agent-Based Model', *Science of the Total Environment*, 595, pp. 159–168. doi: https://doi.org/10.1016/j.scitotenv.2017.03.242

Lau, K.H. and Kam, B.H. (2005) 'A cellular automata model for urban land-use simulation', *Environment and Planning B: Planning and Design*, 32(2), pp. 247–263. doi: https://doi.org/10.1068/b31110

Omidvarfar, S. *et al.* (2021) 'Flood hazard zoning and assessment in Tabriz city using Fuzzy AHP model', Second International Conference and Fifth National Conference on Conservation of Natural Resources and Environment, Ardabil. Available at: https://doi.org/https://civilica.com/doc/1248903 (Accessed date: 10 July 2026).

Rabori, A.M. and Ghazavi, R. (2018) 'Urban flood estimation and evaluation of the performance of an urban drainage system in a semi-arid urban area using SWMM', *Water Environment Research*, 90(12), pp. 2075–2082. doi: https://doi.org/10.2175/106143017X15131012188213

Rossman, L.A. and Huber, W.C. (2021) *Storm Water Management Model Reference Manual Volume I – Hydrology (Revised)*. Cincinnati, OH: U.S. Environmental Protection Agency. Available at: https://cfpub.epa.gov/si/si_public_record_report.cfm?Lab=NRMRL&dirEntryId=309346 (Accessed: 10 July 2026).

Sun, N. *et al.* (2014) 'Impact of SWMM catchment discretization: Case study in Syracuse, New York', *Journal of Hydrologic Engineering*, 19(1), pp. 223–234. doi: https://doi.org/10.1061/(ASCE)HE.1943-5584.0000777

Taghizadeh, S., Khani, S. and Rajaee, T. (2021) 'Hybrid SWMM and particle swarm optimization model for urban runoff water quality control by using green infrastructures (LID-BMPs)', *Urban Forestry & Urban Greening*, 60, p. 127032. doi: https://doi.org/10.1016/j.ufug.2021.127032

White, R. and Engelen, G. (1993) 'Cellular automata and fractal urban form: A cellular modelling approach to the evolution of urban land-use patterns', *Environment and Planning A*, 25(8), pp. 1175–1199. doi: https://doi.org/10.1068/a251175

Zhang, B., Xie, G., Zhang, C. and Zhang, J. (2012) 'The economic benefits of rainwater-runoff reduction by urban green spaces: A case study in Beijing, China', *Journal of Environmental Management*, 100, pp. 65–71. doi: https://doi.org/10.1016/j.jenvman.2012.01.015